Monatshefte für Chemie 138, 823–832 (2007)
DOI 10.1007/s00706-007-0669-3
Printed in The Netherlands

Monatshefte für Chemie
Chemical Monthly

Synthesis and DFT Defined *trans*(O_5O_6) Molecular Structure of Cs[Fe(1,3-*pddadp*)] · $2H_2O$. Strain Analysis and Spectral Assignment of the Complex

Zoran D. Matović[1,*], **Vesna D. Miletić**[1], **Miorad M. Vasojević**[1], **Milica Cvijović**[2], **Svetlana Ćurčić**[1], and **Svetlana K. Belošević**[1]

[1] Department of Chemistry, Faculty of Science, University of Kragujevac, Kragujevac, Serbia
[2] Faculty of Agronomy, University of Kragujevac, Čačak, Serbia

Received November 26, 2006; accepted (revised) February 20, 2007; published online May 31, 2007

Summary. An iron(III) complex with the hexadentate ligand 1,3-propanediamine-*N*,*N*′-diacetate-*N*,*N*′-di-3-propionate (1,3-*pddadp*) was prepared, chromatographically isolated as its isomer *trans*(O_5O_6)-Cs[Fe(1,3-*pddadp*)] · $2H_2O$, and characterized. The *trans*(O_5O_6) configuration of the iron(III) compound was found to dominate and this geometry was established by means of IR spectroscopy and Density Functional Theory (DFT). Structural data correlating the octahedral geometry of the [Fe(1,3-*pddadp*)]$^-$ unit and an extensive strain analysis are discussed in relation to the information obtained for similar complexes. Antibacterial activities of the free ligand and its corresponding iron(III) complex towards common *Gram*-negative and *Gram*-positive bacteria are reported as well.

Keywords. Iron(III) complexes; Aminopolycarboxylates; DFT; Strain analysis; Antibacterial activity.

Introduction

Aminopolycarboxylate chelates have a very wide application in coordination chemistry. Their use in analytical chemistry is well-known. There is an ongoing interest in their use as scavengers for species such as NO in environmental applications [1]. In addition, iron ions participate in the conversion of molecular oxygen to highly reactive and damaging species, such as hydroxyl radicals, which are believed to form by *Fenton* or *Fenton*-like chemistry; chelating iron in inactive form, has been considered to be one of the most important ways to inhibit the damage by the reactive species [2–5].

The *edta*-like ligands (diamine-*N*,*N*′-diacetate-*N*,*N*′-di-3-propionate ions (*eddadp* or 1,3-*pddadp*)), differing only in the length of the diamine chain, can form a maximum of three geometrical isomers upon hexadentate coordination: *trans*(O_5) (**I**), *trans*(O_5O_6) (**II**), and *trans*(O_6) (**III**) (Fig. 1) (O_5 and O_6 refer to the five- and six-membered N–O rings). The ethylenediamine-*N*,*N*,*N*′,*N*′-tetraacetate ion (*edta*$^{4-}$) can be (but often is not) hexadentate to transition metal ions forming coordination octahedral with C_2 symmetry. Bonding parameters that greatly influence the coordination number of metal ions in *edta* and *edta*-type complexes have been discussed by *Yamamoto et al.* [6]. When ionic radii of the metal is larger than 0.79 Å and the *d*-electron configuration is other than d^0, d^5, or d^{10}, the *edta* ligand might be pentadentate with a monodentate ligand occupying the sixth position; and if the metal ion has 0, 5, or 10 *d*-electrons with an ionic radii that exceeds 0.79 Å then its coordination number might increase from 6 to 7 or 8. The high-spin iron(III) ion with an ionic radius of 0.79 Å and a d^5-electron configuration forms usually seven-coordinate [7] complexes with a hexadentate *edta* ligand. This feature implies that the Fe(III) ion is slightly to big to be encircled in an octahedral environment by *edta*$^{4-}$ capable of forming five-membered rings only.

---

[*] Corresponding author. E-mail: zmatovic@kg.ac.yu

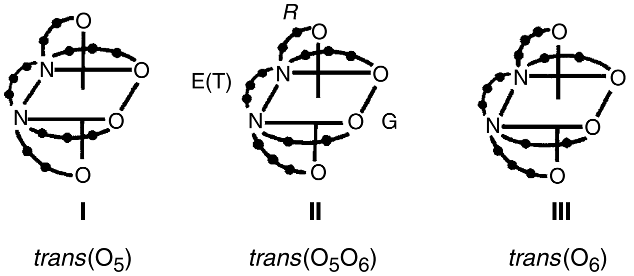

Fig. 1. Three possible geometrical isomers of hexadentate [M(1,3-*pddadp*)]$^{n-}$ complexes

In [Co(*edta*)]$^-$ [8, 9] the ethylenediamine ring and two of the glycinate rings occupy what conventionally has been called the equatorial or girdling plane and have been designated as the E or G rings. The other two glycinate rings (out-of-plane or R rings) coordinate axially. In these kinds of complexes the E ring and the two in-plane G rings are more strained than the two R rings coordinated axially. The *edta*-like ligands with longer (diamine or carboxylate) chains are likely to function as hexadentate ligands with metal ions of different size [10]. Such ligands (*eddadp* or *pddadp*) ease away any in-plane strain, thus allowing the complexes to attain octahedral angles closer to the ideal with apparently less strain in the M–L bonds by forming less-strained isomers as evidenced in their molecular structures [11, 12]. The six-membered β-alaninate rings of *eddadp* serve better for the formation of less-strained G rings favoring the *trans*(O_5) isomer of [M(*eddadp*)]$^{n-}$ complexes [10–12]. Only one *trans*(O_5) isomer was also prepared with the optically active (S,S)-*edds* ligand ((S,S)-ethylenediamine-N,N'-disuccinate ion) which produces metal complexes stereospecifically with the Λ configuration [12]. Contrary to this, all three possible isomers of the [M(1,3-*pddadp*)]$^{n-}$ have been reported for Cr(III) [13], but only two isomers (*trans*(O_5O_6) and *trans*(O_6) for Co(III) [14, 15] and *trans*(O_5) and *trans*(O_5O_6) for Rh(III) [16]) have been isolated and characterized. In addition, only one dominant isomer of the same complex *trans*(O_5) for Ni(II) [10] and *trans*(O_6) for Cu(II) [17] has been isolated. Therefore, Fe(III) ion forms octahedral six-coordinate complexes with *eddadp* (*trans*(O_5) isomer only) and (S,S)-*edds* (*trans*(O_5) isomer only) ligands unlike the *edta*$^{4-}$ complex which is usually seven-coordinate with the seventh coordination site occupied by the molecule of water [6, 7].

Theoretical calculations provide insight into the structural and electronic properties of the metal complexes, but accurately determining relative energies for the high- or low-lying spin states accessible to open-shell Fe(III) complexes is a computational challenge. The reliability of predicting spin state differs among common computational approaches. *Ab initio Hartree Fock* theory (*HF*) tends to favor high spin, HS, whereas pure DFT functionals favor low spin, LS; a compromise can be reached with the use of hybrid DFT functionals which include *HF* exact exchange [18]. *B3LYP* [19] has been one of the most successful and widely used hybrid functionals for transition metal properties. However, *B3LYP* has still been shown to favor HS states, therefore energetically and completely reliable predictions are still not within reach [20–23]. *Deeth* and *Fay* compared various DFT functionals in their ability to reproduce spin states of iron(II) and iron(III) confirming again that pure DFT functionals favour LS states but stressed RPBE functional to be the best choice to reach the realistic spin state energies [18]. More recently, there have been studies involved in an evaluation of DFT functional OPBE, which combines *Handy*'s optimized exchange (OPTX) [24] with the PBE correlation [25], where have been shown OPBE to correctly predict the spin states (singlet through sextet) [26, 27]. The same work indicated that standard DFT functional *BLYP* [28, 29], exerted good agreement between theoretically calculated and the experimentally obtained geometries [26, 27].

Very recently, *Meier et al.* reported solid state and solution structural and DFT investigation of the Fe(III) bis-*mida* complex [Fe(III)(*mida*)$_2$]$^-$ (*mida* = N-methyliminodiacetate) [30]. DFT chemical calculations of all three possible configurations of the [Fe(*mida*)$_2$]$^-$ complex ion in the gas phase supported the finding that the *mer* isomer is more stable than the u-*fac* (*cis*) and s-*fac* (*trans*) isomers. They carried out fragment analysis on the [Fe(*mida*)$_2$]$^-$ ion for each isomer and deduced the s-*fac* isomer of [Fe(*mida*)$_2$]$^-$ to be the least stable one because of the weakest metal-ligand interactions and the highest ligand strain [30].

In this work the ionic [Fe(*pddadp*)]$^-$ complex with *trans*(O_5O_6) geometry has been prepared and characterized. The infrared (carboxylate region) spectra of [Fe(*pddadp*)]$^-$ and room temperature magnetic moment were recorded and discussed in relation to the structure of the complexes. This work aims also to elucidate the different geometrical isomers and electronic structures, by DFT computations, of not only the [Fe(*pddadp*)]$^-$ complex but also other similar [Fe(*L*)]$^-$ complexes ($L = eddadp$ and (*S*,*S*)-*edds*).

Results and Discussion

The ligand 1,3-*pddadp* (1,3-propanediamine-*N*,*N*′-diacetate-*N*,*N*′-di-3-propionate ion) having mixed five- and six-membered carboxylate arms was found to minimize the strain of the chelate system by forming isomers that have six-membered rings in the G plane. The ligand H_4-1,3-*pddadp* was prepared by the well known condensation method between 1,3-propanediamine and neutralized chloroacetic and 3-chloropropanoic acids [14]. As was expected, the six-membered 3-propionate chelate serves better for the formation of less-strained G rings. This was the case in many synthetic reactions and the dominant *trans*(O_5) geometry (Fig. 1 isomer **I**) was verified crystallographically for the complexes of Rh(III) [31] and Ni(II) [10]. What was unexpected in hexadentate [*M*(*pddadp*)]$^{n-}$ complexes (*M* = Cr(III), Co(III), and Cu(II)) is that the dominant isomer was found to be *trans*(O_6) [13, 15, 17] with 3-propionate rings in axial positions (Fig. 1 isomer **III**). On the other hand, the *trans*(O_5O_6) geometry has been also found for Co(III) [14] and Rh(III) [31]. Based on the metal ion size [Co(III) < Cr(III) < Fe(III) < Rh(III) < Ni(II)] and the presence of strain in the G plane the formation of the *trans*(O_5) isomer might be expected to be more strongly favored for Rh(III) and Ni(II) than for Co(III) and Cr(III). In case of Fe(III) all three isomers, according to the metal size, might be expected. Actually, we isolated chromatographically only one isomer of the Cs[Fe(*pddadp*)] $\cdot$ $2H_2O$ complex. The *trans*(O_5O_6) geometry has been established by means of using DFT theory implemented in the ADF software package and comparing the obtained results with spectroscopic (IR) data.

ADF (Amsterdam Density Functional) is a Fortran program for calculations on atoms and molecules [32–34]. It can be used for the study of Fe(III) complexes [26, 27]. The underlying theory is the *Kohn-Sham* approach to the Density Functional Theory (DFT). This implies a one-electron picture of the many-electron systems but yields in principle the exact electron density (and related properties) and the total energy. For the searching of optimal geometry we have chosen *Becke* exchange and *LYP* correlation gradient corrections (also called *BLYP*) [28, 29]. In each case we tried to optimize geometries of all the hypothetic geometrical isomers (*trans*(O_5), *trans*(O_5O_6), and *trans*(O_6), see Fig.1). As a first step we pre-optimized particular isomers by molecular mechanics MM$^+$ (Hyperchem7.01 [35]) and then left the structures to be optimized by ADF2006.01. In case where we had crystal structures (*eddadp* and (*S*,*S*)-*edds*) we used them directly for optimization. The systems were treated within the unrestricted formalism for $S = 1/2$, $3/2$, and $5/2$. For this purpose we used OPBE functional [24, 25] starting from *BLYP* optimized structures. The complexes were left for full optimizations without restrictions (symmetry, restrains, or constrains). All the possible geometrical isomers of [Fe(*L*)]$^-$ complexes (*L* = *eddadp*, (*S*,*S*)-*edds*, and *pddadp*) were examined here and

Table 1. Relative energies (calculated by ADF) (kJ/mol) correlating different isomers of octahedral Fe(III) *edta*-type complexes

Geometrical isomer	[Fe(*eddadp*)]$^-$			[Fe((*S*,*S*)-*edds*)]$^-$			[Fe(*pddadp*)]$^-$		
	$S = 1/2$	$S = 3/2$	$S = 5/2$	$S = 1/2$	$S = 3/2$	$S = 5/2$	$S = 1/2$	$S = 3/2$	$S = 5/2$
				BLYP					
trans(O_5)	15.15	44.60	0	3.68	64.00	0			7.74
trans(O_5O_6)			13.26			b	26.44	55.73	0
trans(O_6)			268.28			b			b
				OPBE					
trans(O_5)	20.16	20.06	0	72.89	77.49	0			6.45
trans(O_5O_6)			15.37			b	107.19	80.69	0
trans(O_6)			302.78			b			20.49

[a] The isomer with the lowest total energy has been indicated with 0 kJ/mol

[b] Extremely poor SCF convergence

their relative energy values obtained for different spin multiplicity *S* (doublet, quartet, and sextet state) are reported in Table 1. Relative energies are obtained from the calculated total energies without subtracting BSSE as it is not very large with DFT, and certainly not with the TZ2P basis set. Evidently the sextet state, $S = 5/2$, is the most stable one in all examined cases.

The room temperature magnetic moment value for $\text{Cs[Fe(}pddadp\text{)]} \cdot 2\text{H}_2\text{O}$ is 5.78 BM (see Experimental). This is consistent with magnetic moment values found in other octahedral complexes with $S = 5/2$. The excellent agreement between the computational predictions for $S = 5/2$ and the experimental data is apparent, also considering that the theoretical calculation is able to correctly discriminate, on the basis of the energy values, among the different spin states [26, 27]. Therefore, we decided not to examine all the spin states of $[\text{Fe}(L)]^-$ complexes but only $S = 5/2$ for the less stable geometric isomers and all the spin states (1/2, 3/2, and 5/2) for the most stable isomer (Table 1). This is, HS–LS energy gap study is not supposed to be the primary goal in this paper but only to correlate and confirm spin state in case of Fe(III)-*edta*-type framework.

It is also evident that DFT calculations gave the *trans*(O_5) geometry as the most stable one in case of Fe-*eddadp* and predict the same geometry in case of Fe-(*S*,*S*)-*edds*. However, in our case, DFT data favors the *trans*(O_5O_6) isomer as it lies lower on energy scale by 7.74 kJ/mol than the *trans*(O_5) one. An energy difference of 20.49 kJ/mol for *trans*(O_6) isomer (using OPBE functional) indicates that influence of the metal ion size and ligand configuration move an Fe(III) ion to the Ni(II) and Rh(III) side. One rationale approach to explain this energy order is to presume that the presence of *trans*(O_5) and *trans*(O_5O_6) isomers are possible (due to low energy difference) and *trans*(O_6) is excluded from a reaction mixture. Therefore, we assigned *trans*(O_5O_6) geometry to the isolated $[\text{Fe(}pddadp\text{)}]^-$ complex. But, why we are so sure that this assignment is correct? There are several reasons for this:

a) First, the predictions about the favored isomer in case of Fe-*eddadp* and Fe-(*S*,*S*)-*edds* are true and in excellent agreement with experimental data [6, 30, 36]. The energy difference between the first two isomers range from 7.44 kJ/mol in case of Fe-*pddadp* to 13.26 kJ/mol in case of Fe-*eddadp*

Table 2. Structural parameters correlating experimental and ADF data of octahedral Fe(III) *edta*-type complexes

Structural parameters	[Fe(*eddadp*)][a]		[Fe((*S*,*S*)-*edds*)][b]		[Fe(*pddadp*)]	
	Exp	*BLYP*	Exp	*BLYP*	*BLYP*	COSMO
d(Fe–N)/Å, G plane	2.198	2.379	2.103	2.319	2.462	2.417
	2.205	2.369	2.149	2.318	2.405	2.332
d(Fe–O)/Å, G plane	1.949	1.935	1.971	1.939	1.965	1.994
	1.930	1.938	1.984	1.941	1.928	1.962
d(Fe–O)/Å, R	2.001	2.041	1.986	2.065	2.044	2.060
	2.004	2.036	2.047	2.065	1.997	1.994
cis angles/°, G plane						
N–Cu–N	81.9	79.7	82.1	76.7	87.7	88.1
O–Cu–O	100.2	108.7	99.7	111.3	105.3	103.1
N–Cu–O	90.0	86.0	90.4	86.6	77.2	77.5
	89.9	86.1	88.9	86.5	90.0	91.4
cis angles/°, RG plane						
N–Cu–O	90.7	83.1	95.8	88.7	83.2	86.2
	92.2	82.8	93.2	88.8	84.2	89.8
trans angles/°, G plane	165.6	164.5	169.7	161.1	162.8	162.0
	166.2	164.4	166.8	161.0	177.2	179.1
trans angles/°, R	168.3	152.6	169.0	158.2	155.9	164.3
RMS overlay error/Å[c]	0.0987		0.1078			

[a] Ref. [6]

[b] Ref. [36]

[c] With respect to overlay of molecules obtained from X-ray data and from DFT theory

(using *BLYP* functional). The ADF calculations in case of Fe-(*S*,*S*)-*edds* for *trans*(O_6) and *trans*(O_5O_6) isomers occurred under extremely poor SCF convergence not allowing these isomers to be optimized. It is to be stated again that the optically active (*S*,*S*)-*edds* ligand produces metal complexes stereospecifically giving only one *trans*(O_5) isomer of the *Λ* configuration [36–38]. All these present reasonable supporting evidence in our case.

b) Second, when we correlated geometry of experimental (X-ray) and DFT data of octahedral Fe(III)-*eddadp* and Fe-(*S*,*S*)-*edds* complexes (Table 2) supporting conclusions are evident. If one compares bond lengths and angles it can be seen from Table 2 that all the data from DFT theory generally well correlate with those found in crystal structure of complexes in question. Exception might be found in in-plane Fe–N bond lengths and out of plane *trans* angles. When we correlate optimized geometries with corresponding X-ray structures in a molecule's overlay fashion the *RMS* errors of 0.0987 in case of Fe-*eddadp* and 0.1078 in case of Fe-(*S*,*S*)-*edds* have been obtained (Table 2). The superimposed structures of investigated complexes are shown in Fig. 2. The Fe–N (equatorial) bond lengths differ from X-ray ones by ∼0.2 Å. On the other hand, in all the complexes DFT investigated Fe–N (equatorial) distances are different among HS and LS states. In general the HS state correlates with long Fe–N (equatorial) bond distances (>2.2 Å). In contrast the LS state correlates with short Fe–N (equatorial) bond distances (<2.10 Å). In other words there is a pronounced effect of spin state on structural parameters. This is consistent with the data published up to date [18, 25, 26, 30]. On the other hand, there are also two other sources of errors or discrepancies: (1) we are computing a gas-phase model system which lacks the molecular environment (solvent or crystal). In the absence of environmental effects, quantum calculations on anions often lead to occupied orbitals having physically unreasonable positive energies but ionization and ligand dissociation is prevented by the finite size of the basis set as pointed out by *Deeth* and *Fey* [18]; and (2) the experimental techniques are also often not that accurate (*e.g.* X-ray is often overrated). As pointed out by the same authors [18] the COSMO solvation (approximation of the complex surroundings with a continuum dielectric field) is a convenient way of mitigating the structural effects of excess charge on transition metal complexes, and we used this approach to re-optimize *trans*(O_5O_6) geometry of Fe-*pddadp*. The SCF exerted so poor convergence in case of Fe-*eddadp* and Fe-(*S*,*S*)-*edds* thus not allowing these molecules to be optimized. Table 2 illustrates that certain improvement in the calculated geometries is achieved in the presence of a solvent continuum dielectric field, but the *M*–*L* distances, as found earlier [18], remain slightly longer ($M\text{–}N = 2.332\text{–}2.417$ Å) than the expected crystal structure averages ($M\text{–}N =$ 2.1–2.2 Å). Further, when equatorial *trans* bond angles are in question there is no substantial improvement. This is, we still deal with quite large N–Fe–O (eq.) angles not observed in other Fe-*edta*-type complexes. However, the axial *trans* O–Fe–O angle reasonably increased from 155.9 to 164.3°.

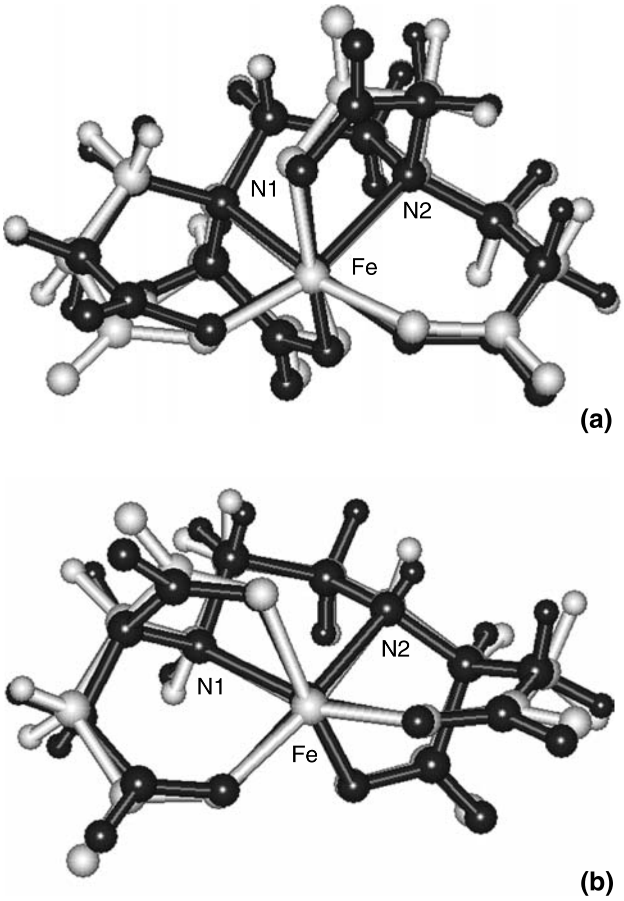

Fig. 2. Overlay of ADF-calculated (white) and X-ray structures (black) of (a) $[Fe(eddadp)]^-$, (b) $[Fe((S,S)\text{-}edds)]^-$ complexes

c) Third, the *trans*(O_5O_6) geometry of Fe-*pddadp* dictates low C_1 molecular symmetry of the complex anion with respect to holohedrized C_2 symmetry of *trans*(O_5) and *trans*(O_6) anions. On the other hand such a C_1 symmetry reflects many substantial features of the corresponding complexes. One of the important properties reflects in a shape of the IR spectrum (carboxylate region). As found for metal aminocarboxylic acid complexes [39, 40] in the asymmetric carboxylate region the asymmetric stretch of five-membered carboxylate moieties lies at higher energy than the corresponding frequency of six-membered carboxylate moieties. The complexes with higher C_2 symmetry exhibit two very strong and well separated bands in the asymmetric stretching carboxylate frequency region which were assigned to carbonyl stretch of 5-membered rings (higher energy) and 6-membered rings (lower energy). The C_1 complex *trans*(O_5O_6) having four non-equivalent rings, exhibits four (in ideal case) absorption bands each belonging to a particular carboxylate arm. In our case the Fe-*pddadp* complex having three non-equivalent rings, instead of four, exhibits three absorption bands: 1653 cm^{-1} at higher energy and 1622 and 1610 cm^{-1} at lower energy (Fig. 3a). These data are in agreement with its C_1 molecular symmetry.

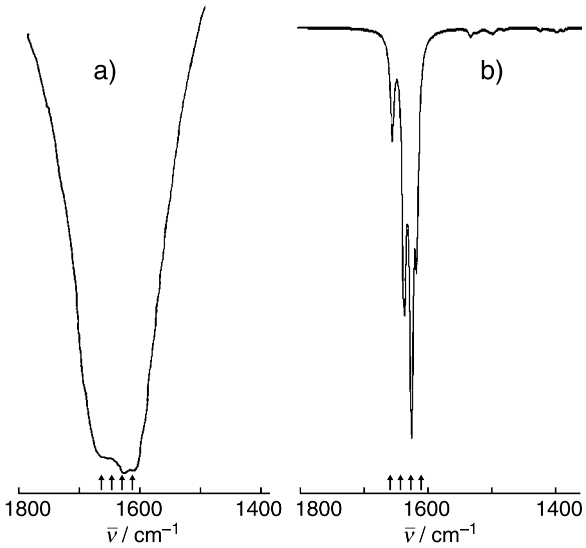

Fig. 3. Portion of the infrared spectra: a) Cs[Fe(1,3-*pddadp*)] · $2H_2O$, b) DFT calculated

We used OPBE functional to run frequency calculation in case of *trans*(O_5O_6) isomer. After a mild scaling correction (1.01; Lorentzian peak width 7.0) the calculated frequencies are in excellent agreement with the experimental values; the predicted infrared intensities are almost qualitatively correct (see Table 3; carboxylate region). The DFT calculated IR spectrum of *trans*(O_5O_6) Fe-*pddadp* shows four absorption bands: 1652 and 1633 cm^{-1} at higher energy and 1622 and 1615 cm^{-1} at lower energy (Fig. 3b) as theory predicts. Table 3 gives the experimentally found and theoretically calculated frequencies and force constants. The small discrepancies in shape, intensities, and the force constants are due to the overlaps and to the lack of the molecular environment.

The band which appeared at higher energy corresponds to the asymmetric stretch of coordinated carboxylates contained in a glycinate residue (R and G rings) and that two at lower energy were assigned to the moieties of the six-membered carboxylate arms. This is confirmed by the careful inspection of the vibrational modes of DFT calculated frequencies. It is to be noted that five-membered higher energy bands comprise ~15% COO vibration mode of six-membered rings and *vice versa*. The spectral analysis and comparison of the experimental and DFT calculated spectra provide further strong supporting evidence with respect to our doubt whether to accept or not *trans*(O_5O_6) isomer as the most favorable one in case of [Fe(*pddadp*)]$^-$ anion.

Table 3. Experimental and DFT calculated infrared frequencies (carboxylate region), force constants, and intensities of *trans*(O_5O_6) [Fe(*pddadp*)]$^-$ complex

Assignment	Frequency / cm^{-1}		Force constant / mDyn $Å^{-1}$		Intensity / km mol^{-1}	
	Experimental	DFT	Experimental	DFT	Experimental	DFT
$\bar{\nu}_{as}$(COO) 5-membered	1653	1652	15.09	17.29	strong	302
$\bar{\nu}_{as}$(COO) 5-membered		1633		16.84		794
$\bar{\nu}_{as}$(COO) 6-membered	1622	1622	14.75	15.07	very strong	1073
$\bar{\nu}_{as}$(COO) 6-membered	1610	1615	14.49	16.41	strong	532

From this place we shall adopt *trans*(O_5O_6) geometry of [Fe(*pddadp*)]$^-$ complex in the same manner as the geometry was determined by an X-ray analysis. We chosed the optimized Fe-*pddadp* molecule calculated by the COSMO solvation model as such structural perfomances are slightly better in this case than those obtained from gas-phase calculation. So let us keep our attention on a spatial shape of *trans*(O_5O_6) [Fe(*pddadp*)]$^-$ anion defined by ADF software package (Fig. 4). The *trans*(O_5O_6) [Fe(*pddadp*)]$^-$ anion contains a Fe(III) ion in a distorted octahedral N_2O_4 environment. In the spatial structure (see Fig. 4) the iron(III) ion coordinates six donor atoms from the ligand: four deprotonated carboxylic oxygens and two amine nitrogen atoms. The distances are within the range 1.962 and 2.418 Å (see Table 2) and comparable with those obtained for related diamino *edt*-type complexes [6, 36–38] except, as mentioned before, longer in-plane Cu–N distances. The *cis* angles at the iron(III) ion range from 77.5 to 103.1° and the *trans* angles from 162 to 179.1° showing moderate distorsion. The 5-membered glycinato chelation rings adopted an twisted-envelope conformation. The 6-membered rings: backbone 1,3-propanediamine and two β-alaninato (G, R), have been found in skew-boat conformation. All these structural data are in accordance with those found in X-ray structures of similar complexes (Table 2).

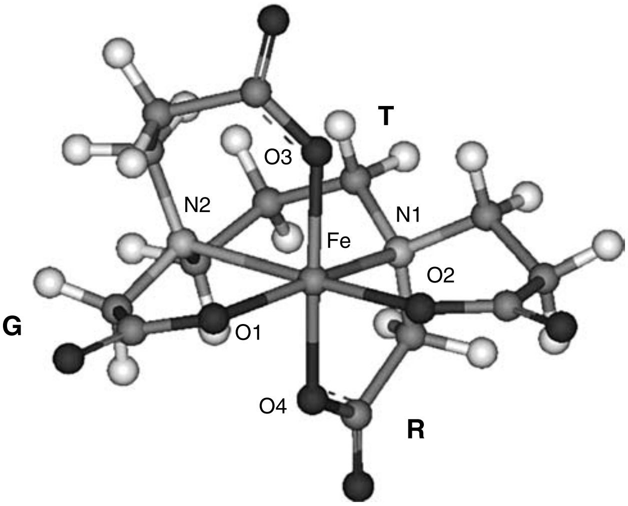

Fig. 4. Spatial view of DFT-COSMO calculated molecular structure of *trans*(O_5O_6)-[Fe(1,3-*pddadp*)]$^-$ ion

The indication of strain for iron(III) complexes might be considered in terms of:

(i) the *cis* and *trans* angles around the central ion;
(ii) the ring angle sums of the various kind of rings;
(iii) the Cu–O–C or Cu–N–C bond angles;
(iv) the bond angles that the coordinated nitrogen atom makes with its connectors.

Strain analysis data are available for the *trans*(O_5O_6)-[Rh(1,3-*pddadp*)]$^-$ complexes [16].

Table 4. Strain analysis of metal complexes with *edta*-type ligands containing mixed five- and six-membered carboxylate rings

Complex	$\Sigma\Delta(O_h)$/°[a]	$\Delta\Sigma$(ring)/°[b]			$\Delta(M\text{–O–C})$/°[c]		$\Sigma\Delta$(N)/°[d]	Δ(A)/Å[e]	Ref.
		E(T)	R	G	R	G			
trans(O_5)-[Fe(*eddadp*)]$^-$	61	−24	+7	+49	+11	+23	10	0.002	[6]
trans(O_5)-[Fe((*S*,*S*)-*edds*)]$^-$	59	−23	−20	+36	+5	+21	60	0.061	[36]
trans(O_5)-[Rh(*pddadp*)]$^-$	55	+37	−6	+27	+5	+14	17	0.016	[16]
trans(O_5)-[Ni(*pddadp*)]$^{-2}$	60	+28	0	+36	+7	+20	8	0	[10]
trans(O_5O_6)-[Fe(*pddadp*)]$^-$	56	+24	+1	+1	+20	+20	12	0.066	this work
			+43	+50					
trans(O_5O_6)-[Rh(*pddadp*)]$^-$	42	+33	1	−10	+10	+13	13	0.020	[16]
			+32	+41					
trans(O_6)-[Co(*pddadp*)]$^-$	38	+28	+33	−11	+17	+14	16		[15]
trans(O_6)-[Cr(*pddadp*)]$^-$	42	+26	+33	−11	+19	+5	15		[10]
trans(O_6)-[Cu(*pddadp*)]$^{-2}$	43	+27	+14	−11	0	+5	17	0	[17]

[a] $\Sigma\Delta(O_h)$ is the sum of the absolute values of the deviations from 90° of the $L\text{–}M\text{–}L'$ bite angles. All values rounded off to the nearest degree

[b] $\Delta\Sigma$(ring) is the deviation from the ideal of the corresponding chelate rings' bond angles sum

[c] $\Delta(M\text{–O–C})$ (ring) is the mean value of the deviation of the corresponding rings' M–O–C bond angle from the 109.5°

[d] $\Sigma\Delta$(N) is the sum of the absolute values of the deviations from 109.5° of the six bond angles made by nitrogen atoms. A mean value for the two nitrogens is reported

[e] Asymmetry in tetragonal bonds in Å

Structural data correlating the stereochemistry of $[Fe(\mathit{pddadp})]^-$ with related complexes are given in Table 4.

The total deviation of the octahedral angles of these complexes varies reflecting their large ionic radii and the geometry of the complex (the ring system in the G-plane). These values were obtained: from 55° for Rh-*pddadp* to 61° for Fe-*eddadp* (*trans*(O_5) isomers); from 42° for Rh-*pddadp* to 56° for Fe-*pddadp* (*trans*(O_5O_6) isomers); from 42° for Cr-*pddadp* to 43° for Cu-*pddadp* (*trans*(O_6) isomers). The values are smaller for complexes of Co and Cu (5-6-5 ring system) and these complexes attain higher octahedral symmetry. For metal ions of the size comparable with Fe(III), as was reported in Ref. [10], the best combination of the rings that can span the girdle plane seems to be the 5-6-6 system which allows the diamine ring to adopt the energetically favored *twist* conformation and brings the $O(G_1)$–Fe–$O(G_2)$ *cis* angle close to 90°.

After gas-phase DFT optimized *trans*(O_5O_6) isomer was re-optimized by the COSMO model, the total deviation of the octahedral angles sum decreased from 92 to 56° for Fe-*pddadp* adopting the *quasi* same values as Fe-*eddadp* (61°) and Fe-(*S*,*S*)-*edds* (59°). This continues to follow the trend of slight to moderate deviations of six octahedral angles around the Fe(III) ion leaving corresponding molecules at the same level of distorsion (Table 4).

The bond angle chelate-ring sums for the R, G, and diamine (T) rings are as expected for these kinds of chelates [11, 12, 41] (Table 4). The bond angle chelate-ring sums for the R and G glycinate rings are closer to the ideal values (538.5°) (a total deviation of 1°). The larger deviations are positive for all six-membered rings (Table 4). The diamine (T) rings are in a *twist-boat* conformation and show positive total deviation (from +24° for Fe-*pddadp* to +37° for *trans*(O_5)-Rh-*pddadp*). The total deviations of the β-alaninate rings vary from +14 to +43° (for the R rings) and from +27 to +50° (for the G rings). All complexes considered (Table 4) show positive deviation of the *M*–O–C (R, G) bond angles (except for the tetragonally elongated complex Cu-*pddadp*, Cu–O–C(R) = 109.0 [17]). These deviations, as expected [11, 12, 41], are less for the glycinate rings than for the β-alaninate rings (Table 4).

When each of the deviations for the six angles made by nitrogen atoms is summed up, the total deviations (absolute values) for each complex were obtained (Table 4). Total deviation about the chelating N atoms range from 8° (for Ni-*pddadp*) to 60° (for Fe-(*S*,*S*)-*edds*). These complexes, having N atoms connecting mixed (one acetate and one β-alaninate) rings, with respect to those containing N atoms connecting two acetate or two β-alaninate rings show less total deviations about the N atoms. Comparing these values it is worth-wile to state, the larger deviation about N tetrahedra, the more pronounced octahedral distorsion.

Antimicrobial Tests

Free H_4-*pddadp* ligand and corresponding $Cs[Fe(1,3\text{-}\mathit{pddadp})] \cdot 2H_2O$ complex exerted average influence ($\mathit{MIC} = 40\text{–}90\ \mu g/cm^3$) on microbial growth comparing to the influence of the drug norflotacin taken as a standard ($\mathit{MIC} = 0.5\text{–}12\ \mu g/cm^3$). Chelating effect of H_4-*pddadp* and oxidizing power of Fe(III) from $Cs[Fe(1,3\text{-}\mathit{pddadp})] \cdot 2H_2O$ might be responsible for somewhat greater antibacterial activity than those of recently reported tetradentate amidocarboxylate Cu(II) complexes [42].

Experimental

General Methods

Carbon, hydrogen, and nitrogen analyses were performed with a Carlo Erba EA1108 elemental analyser; their results agreed favorably with calculated values. IR spectra in the 400–4000 cm^{-1} region were recorded on a Perkin Elmer FTIR spectrophotometer Spectrum One, using the KBr pellets technique. Electronic absorption spectra were recorded on a Perkin Elmer Lambda 35 spectrophotometer. For these measurements $1 \times 10^{-3}\ M$ aqueous solutions of the complexes under investigation were used. Magnetic susceptibility measurements were carried out using the *Gouy* method at room temperature. The molar susceptibilities were corrected for the diamagnetism of the component atoms by the use of *Pascal*'s constants.

Starting Materials

1,3-Propanediamine-*N*,*N*′-diacetic-*N*,*N*′-di-3-propionic acid (H_4-1,3-*pddadp*) was prepared according to a published procedure following the condensation method starting from neutralized chloroacetic and 3-chloropropionic acids and 1,3-propanediamine [14]. Reagent grade, commercially available, chemicals were used without further purification. 1,3-Propanediamine, 3-chloropropionic and chloroacetic acids were purchased from Fluka and used as supplied.

General Procedure for the Preparation of Cesium(1,3-propanediamine-N,N′-diacetato-N,N′-di-3-propionato) ferrate(III) dihydrate, $Cs[Fe(1,3\text{-}pddadp)] \cdot 2H_2O$

To a slurry of 20 mmol salt-free $Fe(OH)_3$ was added 6.67 g (20 mmol) H_4-1,3-*pddadp* and the mixture was stirred at 70–

80° for 2 h. To the resulting orange solution ($pH = 2$) sufficient solution of $LiCO_3$, 0.74 g (10 mmol) in 10 cm^3 water, was added to rise the *pH* to 5–6. The resulting solution was poured into a 35 × 5 cm column containing Sephadex QAE A-25 anion-exchange resin in the Cl^- form. The column was then eluted with 0.1 *M* solution of CsCl. Only one light yellow colored band was obtained. The eluate was evaporated to 20 cm^3 at room temperature and desalted by passage through a G-10 Sephadex column, with distilled water as the eluent. After that the eluate was concentrated to a volume of 15 cm^3, ethanol was added, and left in the refrigerator for several days to crystallize as yellow polycrystalline powder. The precipitate was filtered off and washed with ethanol and ether. Yield 5.85 g (56%) $Cs[Fe(1,3\text{-}pddadp)] \cdot 2H_2O$; mp 258°C; Magnetic moment: $\mu_{eff} = 5.78$ BM; UV-Vis data: $\lambda_{max} = 8996$, 12980, 20610, 26788 cm^{-1}; IR data: $\bar{\nu}_{as}(COO) = 1653$, 1622, 1610 cm^{-1}, $\bar{\nu}_s(COO) = 1368$ and 1324 cm^{-1}.

Antibacterial Tests

Antibacterial activities of norflotacin (standard), the free *pddadp* ligand, and the corresponding iron(III) complex were evaluated against human pathogenic *Gram*-negative (*E. coli* ATCC 25922, *Pseudomonas aeruginosa* ATTC 27853), and *Gram*-positive bacteria (*Enterococcus faecalis* ATTC 29212) using the spectrophotometric quantification of microbial growth measuring absorbance at 600 nm [43]. Three to five well isolated colonies of the appropriate bacterial strain were inoculated into *Mueller–Hinton* broth and incubated at 37°C until they reached an optical density (OD600) of 0.08–0.1. The test compounds dissolved in distillated water were used to prepare the tenfold dilution (200, 20, 2, 0.2 $\mu g/cm^3$) in growth media containing bacteria. *Muller–Hinton* broth medium containing inoculated microorganisms were used as a control. Experiments were repeated at least three times to find out reproducibility of the assays. After 24, 48, and 72 h incubation at 37°C the absorbances were determined.

Computational Method

The standard DFT method of quantum chemistry (Amsterdam Density Functional – ADF2006.01) [32–34] with *Vosko-Wilk-Nussair* (*VWN*) parameterization for the Local Density Approximation (LDA) and *Becke* exchange and *LYP* correlation (the *Lee-Yang-Parr* 1988 correlation correction) gradient correction *BLYP* [28, 29] has been used in order to find the optimal geometries of octahedral Fe(III) complexes for each spin multiplicity (doublet, quartet, and sextet). *Handy*'s optimized exchange (OPTX) [24] with the PBE correlation [25] OBPE has been used to increase accuracy of computations of different spin states. No symmetry restrictions were applied. The Fe(III) systems were treated within the unrestricted formalism. The different geometries of the individual chelate systems, starting either from experimental structures (X-ray determined) or MM^+ pre-optimized (Hyperchem7.01 [35]), were optimized until the maximum and the root-mean-squared gradients were below 0.01 and 0.007 Hartree/Å and the maximum and root-mean-squared changes in geometry were below 0.01 and 0.007/Å, respectively. For N, O, and Fe atoms, *Slater*-type orbital (*S*TO) basis sets of triple-ξ quality with two polarization functions (TZ2P type V) from the ADF library have been used and double-ξ quality without polarization functions (DZ type II) in case of H and C atoms. The inner shells were represented by frozen core approximation (1s for C, N, O and 1s-2p for Fe were kept frozen). The subsequent frequency calculations at the same level verified the optimized structures to be ground states without imaginary frequencies. Geometry optimizations without symmetry constraints were performed for *trans*(O_5O_6)-Fe-*pddadp* using the OPBE functional in a COSMO solvation field (*vide infra*). ADF default parameters were used for all the COSMO solvation parameters, together with a non-optimized iron radius $r_{Fe} = 2.02$ Å. As iron is surrounded by six ligands, it is not expected to contribute to the solvent-accessible surface [18]. The frequencies are computed analytically by the use of analytical second derivatives implemented in ADF with integration accuracy 5.

Acknowledgements

The authors are grateful to the Serbian Ministry for Science and Environment protection for financial support (Project No. 142013B).

References

[1] a) Schneppensieper T, Finkler S, Czap A, van Eldik R, Heus M, Nieuwenhuizen P, Wreesmann C, Abma W (2001) Eur J Inorg Chem 491; b) Wolak M, van Eldik R (2002) Coord Chem Rev **230**: 263

[2] Shcherbakova I, Somdeb M, Beer RH, Brenowitz M (2006) Nucleic Acids Research **34**: e48

[3] Changyuan L, Koppenol WH (2005) J Biol Inorg Chem **10**: 732

[4] a) Buda F, Ensing B, Gribnau MCM, Jan Baerends E (2001) Chem Eur J **7**: 2775; (2003) Chem Eur J **9**: 3436; b) Pestovsky O, Stoian S, Bominaar EL, Shan X, Münck E, Que L Jr, Bakac A (2005) Angew Chem Int Ed **44**: 6871

[5] a) Costas M, Mehn MP, Jensen MP, Que L Jr (2004) Chem Rev **104**: 939; b) Anderson VE, Ruszczycky MW, Harris ME (2006) Chem Rev **106**: 3236

[6] Yamamoto T, Mikata K, Miyoshi K, Yoneda H (1988) Inorg Chim Acta **150**: 237

[7] Weyh JA, Hamm RF (1968) Inorg Chem **7**: 2431

[8] Weakliem HA, Hoard JL (1959) J Am Chem Soc **81**: 549

[9] Okamoto K, Tsukihara T, Hidaka J, Shimura Y (1978) Bull Chem Soc Jpn **51**: 3534

[10] Matović ZD, Ianelli S, Pelosi G, Janićijević SK, Ristanović VM, Ponticelli G, Radanović DJ (2002) Polyhedron **21**: 2667

[11] Radanović DJ (1984) Coord Chem Rev **54**: 159

[12] Douglas BE, Radanović DJ (1993) Coord Chem Rev **128**: 139

[13] Kaizaki S, Byakuno M, Hayashi M, Legg JI, Umakoshi K, Ooi S (1987) Inorg Chem **26**: 2395

[14] Radanović DJ, Trifunović SR, Cvijović MS, Maricondi C, Douglas BE (1992) Inorg Chim Acta **196**: 161

[15] Parvez M, Maricondi C, Radanović DJ, Trifunović SR, Miletić VD, Douglas BE (1996) Inorg Chim Acta **248**: 89

[16] Rychlewska U, Djuran MI, Vasojević MM, Radanović DD, Ristanović VM, Radanović DJ (2002) Inorg Chim Acta **328**: 218

[17] Radanović DJ, Prelesnik BV, Radanović DD, Matović ZD, Douglas BE (1997) Inorg Chim Acta **262**: 203

[18] Deeth RJ, Fey N (2004) J Comput Chem **25**: 1840

[19] Becke AD (1993) J Chem Phys **98**: 5648

[20] Reiher M, Salomon O, Hess BA (2001) Theor Chem Acc **107**: 48

[21] Reiher M (2002) Inorg Chem **41**: 6928

[22] Brewer G, Olida MJ, Schmiedekamp AM, Viragh C, Zavalij PY (2006) Dalton Trans 5617

[23] Ghosh A, Tangen E, Ryeng H, Taylor PR (2004) Eur J Inorg Chem 4555

[24] Handy NC, Cohen AJ (2001) Molec Phys 99

[25] Perdew JP, Burke K, Ernzerhof M (1996) Phys Rev Lett **77**: 3865; Erratum **78**: 1396

[26] Swart M, Groenhof AR, Ehlers AW, Lammertsma K (2004) J Phy Chem A **108**: 5479

[27] Swart M, Ehlers AW, Lammertsma K (2004) Molec Phys **102**: 2467

[28] Becke AD (1988) Phys Rev A **38**: 3098

[29] Lee C, Yang W, Parr RG (1988) Phys Rev B **37**: 785

[30] Meier R, Molinier M, Anson C, Powell AK, Kallies B, van Eldik R (2006) Dalton Trans 5506

[31] Helm FT, Watson WH, Radanović DJ, Douglas BE (1977) Inorg Chem **16**: 2351

[32] Velde G te, Bickelhaupt FM, van Gisbergen SJA, Fonseca Guerra C, Baerends EJ, Snijders JG, Ziegler T (2001) J Comput Chem **22**: 931

[33] Fonseca Guerra C, Snijders JG, Velde G te, Baerends EJ (1998) Theor Chem Acc **99**: 391

[34] ADF2006.01, SCM, Theoretical Chemistry, Vrije Universiteit, Amsterdam, The Netherlands, http://www.scm.com

[35] HyperChem(TM), Hypercube, Inc., 1115 NW 4th Street, Gainesville, Florida 32601, USA

[36] Pavelčik F, Kettmann V (1983) Collect Czech Chem Commun **48**: 1376

[37] Pavelčik F, Kettmann V, Majer J (1979) Collect Czech Chem Commun **44**: 1070

[38] Soldanova J, Pavelčik F, Majer J (1981) Acta Cryst **B37**: 921

[39] Nakamoto K, Morimoto Y, Martell AE (1961) J Am Chem Soc **83**: 4528

[40] Ćelap MB, Niketić SR, Janjić TJ, Nikolić VN (1967) Inorg Chem **6**: 2063

[41] Radanović DJ, Ianelli S, Pelosi G, Matović ZD, Tasić-Stojanović S (1998) Inorg Chim Acta **278**: 66

[42] Matović ZD, Miletić VD, Samardžić G, Pelosi G, Ianelli S, Trifunović S (2005) Inorg Chim Acta **358**: 3135

[43] Kavanagh F (1972) In: Kavanagh F (ed) Analytical microbiology, Academic Press, p 44